β-Lactam-Induced Cell Envelope Adaptations, Not Solely Enhanced Daptomycin Binding, Underlie Daptomycin-β-Lactam Synergy in Methicillin-Resistant *Staphylococcus aureus*

Cassandra Lew,[a] Nagendra N. Mishra,[b,c] Arnold S. Bayer,[b,c] Warren E. Rose[a]

[a]School of Pharmacy, University of Wisconsin—Madison, Madison, Wisconsin, USA
[b]The Lundquist Institute-Harbor UCLA Medical Center, Torrance, California, USA
[c]The David Geffen School of Medicine, University of California, Los Angeles (UCLA), Los Angeles, California, USA

ABSTRACT Methicillin-resistant *Staphylococcus aureus* (MRSA) is a serious clinical threat due to innate virulence properties, high infection rates, and the ability to develop resistance to multiple antibiotics, including the lipopeptide daptomycin (DAP). The acquisition of DAP resistance (DAP-R) in MRSA has been linked with several characteristic alterations in the cell envelope. Clinical treatment of DAP-R MRSA infections has generally involved DAP-plus-β-lactam combinations, although definable synergy of such combinations varies in a strain-dependent as well as a β-lactam-dependent manner. We investigated distinct β-lactam-induced cell envelope adaptations of nine clinically derived DAP-susceptible (DAP-S)/DAP-R strain pairs following *in vitro* exposure to a panel of six standard β-lactams (nafcillin, meropenem, cloxacillin, ceftriaxone, cefaclor, or cefoxitin), which differ in their penicillin-binding protein (PBP)-targeting profiles. In general, in both DAP-S and DAP-R strains, exposure to these β-lactams led to (i) a decreased positive surface charge; (ii) decreased cell membrane (CM) fluidity; (iii) increased content and delocalization of anionic phospholipids (i.e., cardiolipin), with delocalization being more pronounced in DAP-R strains; and (iv) increased DAP binding in DAP-S (but not DAP-R) strains. Collectively, these results suggest that β-lactam-induced alterations in at least three major cell envelope phenotypes (surface charge, membrane fluidity, and cardiolipin content) could underlie improved DAP activity, not mediated solely by an increase in DAP binding. (Note that for ease of presentation, we utilize the terminology "DAP-R" instead of "DAP nonsusceptibility.")

KEYWORDS *Staphylococcus aureus*, beta-lactams, cationic peptides, cell membranes

Methicillin-resistant *Staphylococcus aureus* (MRSA) is a problematic pathogen with high associated mortality rates, principally related to its innate virulence properties as well as its ability to evolve resistance to multiple antibiotics (1). The development of clinical MRSA resistance to "last-line antibiotics," including daptomycin (DAP), has been well chronicled, resulting in treatment failures (2–4). DAP's mechanism of action is multifactorial, involving both cell wall synthesis inhibition (5, 6) as well as cell membrane (CM) targeting (7). DAP's CM interaction involves complexing with calcium, oligomeric aggregation, and insertion into the CM as a "functional" cationic peptide (8–10). Accordingly, alterations in genetic pathways responsible for cell envelope homeostasis have been linked to the acquisition of the DAP resistance (DAP-R) phenotype (7, 11, 12).

Several recent clinical studies have utilized combinations of DAP plus selected β-lactams to treat infections caused by DAP-R MRSA (13, 14). The use of such combinations is supported by extensive studies showing *in vitro* synergistic activity, in particular

against MRSA strains resistant to either antibiotic alone (15, 16). Moreover, such combinations may also prevent the development of DAP-R in MRSA strains by forestalling the emergence of single nucleotide polymorphisms (SNPs) in the multiple-peptide resistance factor gene, *mprF*, which is involved in the maintenance of positive surface charge (17). Furthermore, β-lactams can reduce the relative positive surface charge and enhance DAP CM binding in some MRSA strains (18, 19); however, the latter events do not appear to be essential for DAP–β-lactam synergy *in vitro*, suggesting that other mechanisms are in play (20). In addition, as MRSA strains become progressively more resistant to DAP *in vitro* and *in vivo*, they tend to become more β-lactam susceptible (the "seesaw effect") (21). Despite the above-mentioned observations, the precise mechanism(s) responsible for DAP–β-lactam synergy remains incompletely understood (13, 20, 22, 23).

The goal of the current study was to better characterize potential cell envelope mechanisms by which β-lactam antibiotics may promote DAP–β-lactam synergy. We thus delineated several key cell envelope phenotypes in a well-defined set of isogenic DAP-susceptible (DAP-S)/DAP-R MRSA strain pairs ($n = 9$) following exposure to subinhibitory concentrations of selected β-lactams with a broad spectrum of penicillin-binding protein (PBP)-targeting profiles (see below). We focused on those envelope metrics previously associated with DAP-R in MRSA (24, 25), including CM order and surface charge, quantified with and without β-lactam exposure. Moreover, we assessed the role of the CM anionic phospholipid content (predominantly cardiolipin [CL]) and its distribution under the same conditions. Finally, the degree of overall DAP binding was quantified following distinct β-lactam exposures.

(This work was presented in part at the 30th European Congress of Clinical Microbiology and Infectious Diseases [ECCMID] meeting, 18 to 21 April 2020 [26].)

RESULTS

Surface charge. As expected, overall, DAP-R strains exhibited significantly less cytochrome *c* binding at baseline (i.e., elevated cell surface positive charge) (27) than DAP-S strains ($P < 0.05$). Following exposure to all distinct β-lactams (except for cefaclor [CEC]), DAP-S and DAP-R MRSA strains exhibited increased binding to cytochrome *c* (i.e., a more negative relative surface charge than the respective strains with no antibiotic preexposure) (Fig. 1A). Exposure to cloxacillin (LOX) led to the greatest increase in cytochrome *c* binding (more negative surface charge) versus all other β-lactams ($P < 0.05$).

CM order. Exposure to all β-lactams (except for CEC) resulted in more rigid CMs than in untreated strains, in both DAP-S and DAP-R strains (Fig. 1B). Comparing β-lactam treatments to one another, LOX exposure caused the greatest impacts on CM order (more rigidity) ($P < 0.05$) (Fig. 1B).

NAO content. The relative overall *N*-acrylamide orange (NAO) content (as a principal measure of CL, the primary phospholipid [PL]) following β-lactam exposure is shown in Fig. 2A. These data show a general, albeit modest, trend of increased CL contents in both DAP-S and DAP-R strains exposed to this panel of β-lactams, with meropenem (MEM) and LOX being the most impactful.

Anionic phospholipid distribution. We investigated potential differences in anionic phospholipid localizations (predominantly CL) by confocal microscopy in all 9 strain pairs. Confocal images were acquired following growth to the exponential phase, with or without exposure to the selected β-lactams. Fluorescence quantification of the confocal images further validated the apparent increase in the anionic phospholipid content following β-lactam exposure (Fig. 2B). At baseline, DAP-R strains tended to contain more CL per cell than DAP-S strains. In DAP-S strains, all β-lactam exposures led to significantly increased CL contents per cell. In DAP-R strains, exposures to MEM, LOX, or cefoxitin (FOX) led to similarly increased CL contents per cell versus untreated cells ($P < 0.05$).

Figure 3 shows images employing one representative DAP-S/DAP-R strain pair. Before antibiotic exposure, cells showed concentrated CL clusters, which tended to be at either the poles or the cell septal division plane. In contrast, following β-lactam
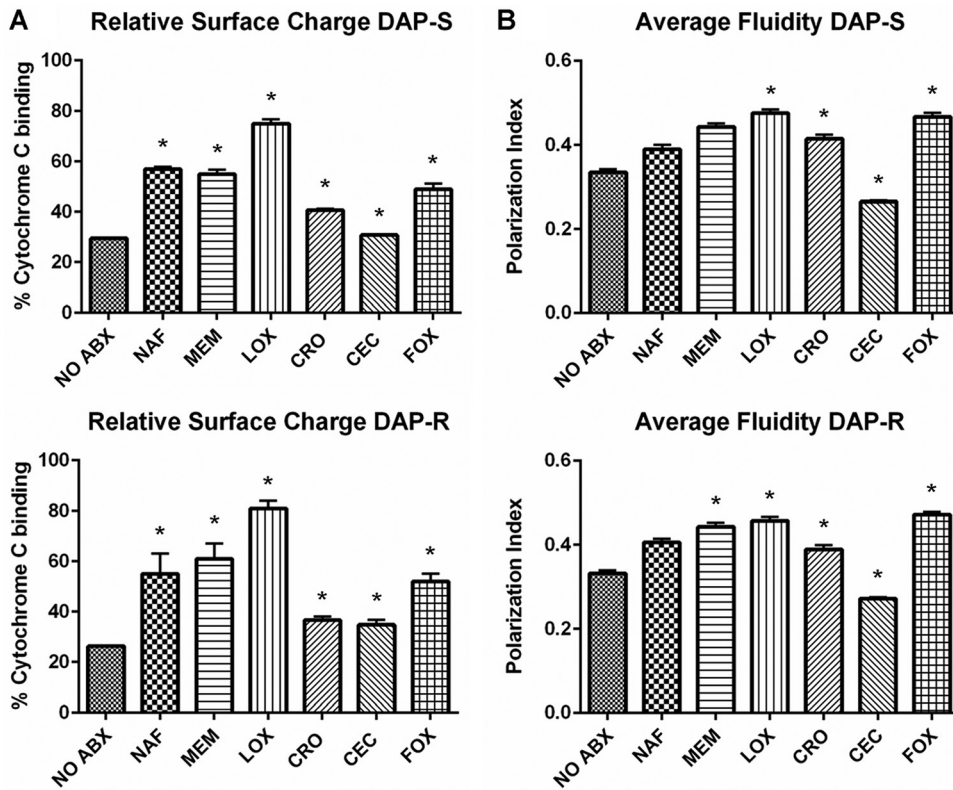
FIG 1 Membrane characteristics previously associated with DAP-R. (A) Relative surface charge of DAP-S and DAP-R strains with or without β-lactam conditioning via a cytochrome c binding assay. A higher percentage of cytochrome c binding indicated a more negative cell surface charge. (B) Membrane fluidity of DAP-S and DAP-R strains with or without β-lactam conditioning via a membrane-polarizing spectrofluorometric assay. The polarization index is inversely correlated with membrane fluidity; i.e., a higher polarization index equates with decreased membrane fluidity. *, $P < 0.05$ versus no antibiotics (NO ABX).

exposures, cells showed a more global, nonseptal distribution of CL around the CM circumference. This perturbed CL distribution was more apparent and distinct in DAP-R than in DAP-S strains.

DAP binding. The binding of BODIPY-DAP was quantified via fluorescence intensity from confocal images, with or without β-lactam exposure. At baseline, DAP-R strains on average actually bound more DAP than their DAP-S counterparts. Among DAP-S strains, exposure to all β-lactams studied yielded significantly increased DAP binding (versus untreated strains) (Fig. 4A) ($P < 0.05$). In contrast, among DAP-R strains, the impact of β-lactam exposures tended to be more variable; thus, nafcillin (NAF) and ceftriaxone (CRO) resulted in significantly decreased DAP binding, while CEC exposure caused significantly increased DAP binding ($P < 0.05$).

Overview of cell envelope parameter impacts of β-lactam exposures. Since clinically, DAP–β-lactam combinations are geared to treat DAP-R MRSA strains, Table 1 summarizes the overall cell envelope alterations identified among our 9 DAP-R strains following β-lactam exposures. Based on the actual data generated, this table lists those cell envelope changes predicted to improve DAP activity.

DISCUSSION

The exact mechanisms underlying the development of DAP-R in MRSA appear to be heterogeneous and multifactorial. Relevant to the current investigation, a number of studies have linked specific alterations in the cell envelope with the acquisition of the DAP-R phenotype (7, 11, 12, 27–29). Clinically, the addition of different β-lactams (e.g., nafcillin and ceftaroline) to DAP treatment has proven effective in many well-characterized cases of recalcitrant MRSA infections caused by DAP-R strains (14, 16, 30). However, the
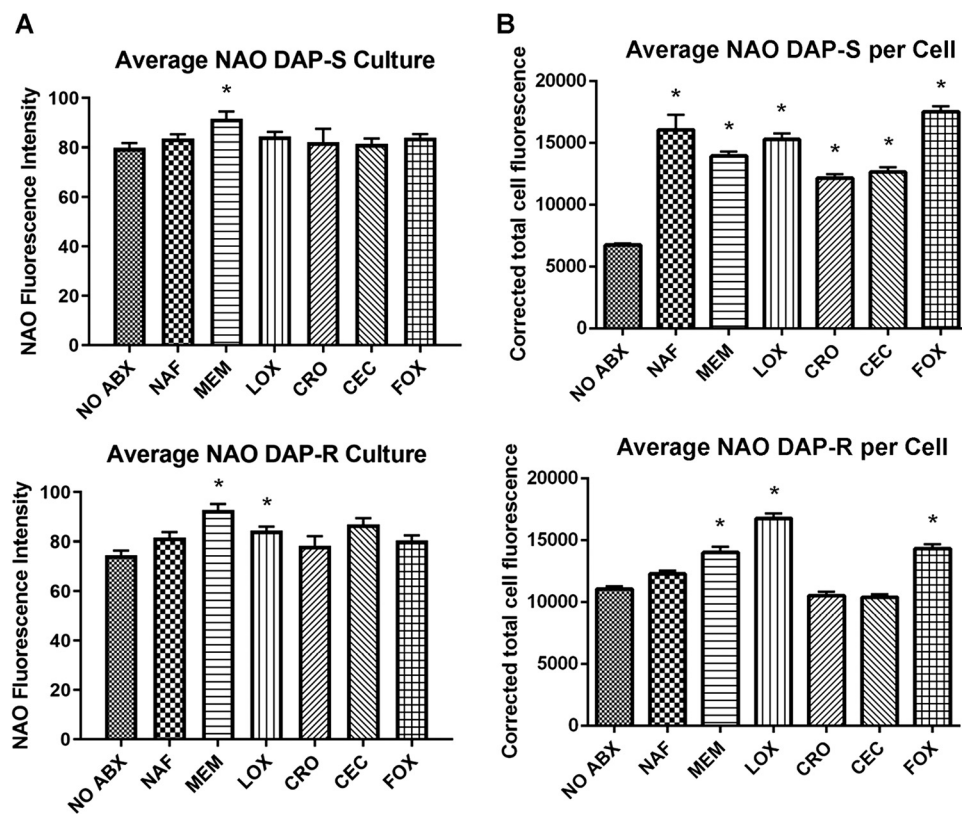
FIG 2 Average anionic PL content quantified by NAO staining (A) and quantification of confocal images (B) of DAP-S and DAP-R strains, with or without β-lactam treatment. *, $P < 0.05$ versus no antibiotics.

mechanism(s) behind the salutary outcomes using these combinations is not well understood. As the cell envelope plays an integral and mechanistic role in DAP's activity, as well as in DAP-R, we hypothesized that β-lactam exposure may lead to CM changes that could potentially enhance DAP's efficacy. Several interesting observations emerged from our analyses.

First, exposures to most (5/6) of the tested β-lactams led to a significant decrease in the relative positive surface charge (versus untreated strains), with LOX being the most impactful in this regard. Of note, previous studies have linked DAP-R with an increased cell surface charge, commonly mediated by either gain-of-function mutations in *mprF* (31, 32) or dysregulation of *dltABCD* expression (11). The resultant increase in the relative positive surface charge was proposed to lead to the repulsion of the bioactive, positively charged DAP-calcium complex (33). The decreased positive surface charge seen in the current study following β-lactam exposures would likely enhance the interaction of the positively charged DAP complex with the cell envelope.

Second, the DAP-R phenotype in MRSA typically correlates with an alteration of membrane order (fluidity/rigidity). One prevailing theme is that an optimal CM order exists for DAP to exert its maximal activity. Thus, DAP-R strains derived either *in vitro* or *in vivo* tend to exhibit extremes of CM order (more rigid or more fluid than the respective DAP-S parental strains) (18). The hypothesis that DAP activity can be influenced substantially by altered CM order was further underscored by Müller et al., who found that DAP binding occurred selectively at more fluid lipid domain sites (34).

In the current investigation, when exposed to β-lactams, our study strains (both DAP-S and DAP-R) generally showed increased rigidity versus their respective non-β-lactam-treated control strains. It seems reasonable to assume that this β-lactam-mediated effect reverts the CM order to a state more favorable for DAP's mechanism of activity. Whether this impact relates to modifications of DAP binding, oligomerization, and/or membrane insertion remains to be determined.
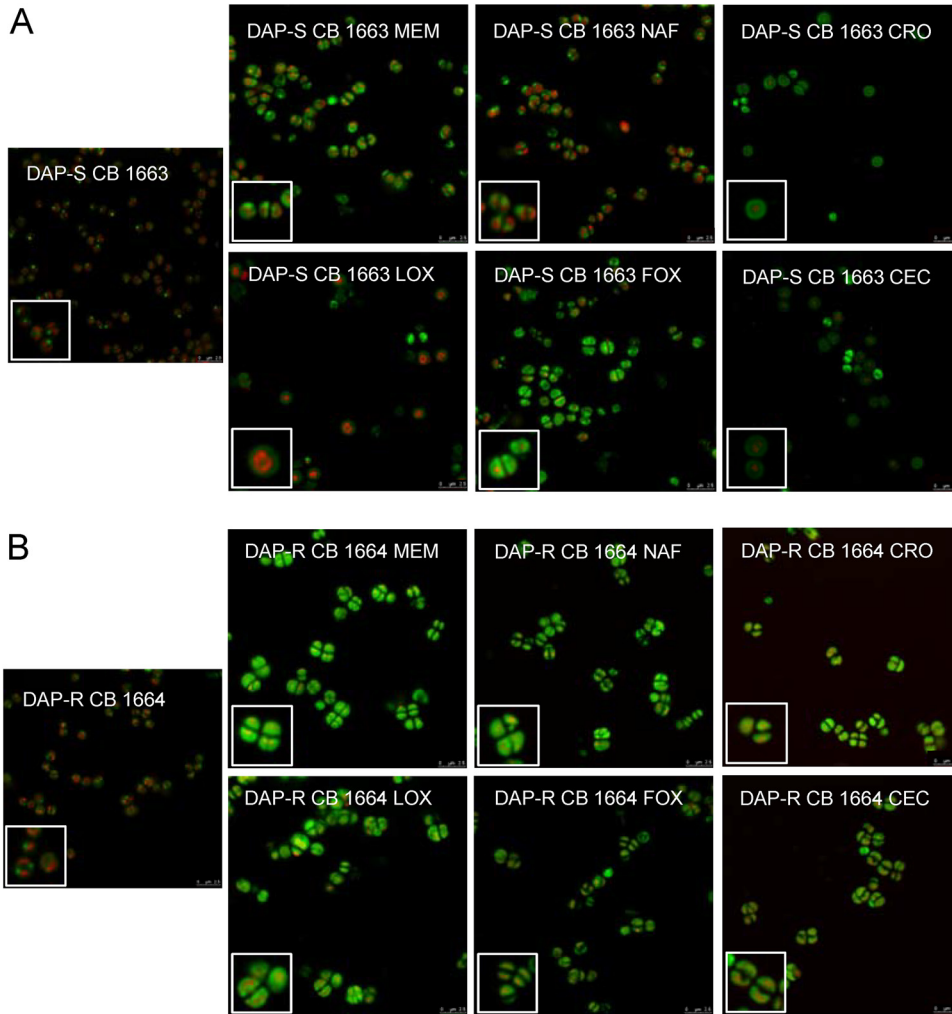
FIG 3 Confocal images of one representative DAP-S/DAP-R strain pair (CB 1663/CB 1664) with or without β-lactam conditioning. NAO was imaged in the green channel, and NucSpot was imaged in the red channel.

Third, the relationship between CL content and distribution with DAP activity has been most well defined among DAP-R enterococci (35). In such strains, CL appears to delocalize from the divisome and redistribute more globally throughout the CM. In the present study, an overall increase in CM CL was observed following β-lactam exposures. It is possible that such CL increases could contribute to a decreased surface charge, with enhanced DAP activity related to increased surface attraction. However, such increases in CL could also result in a compensatory decrease in the CM concentration of phosphatidylglycerol (PG), both an initial anionic anchoring point for DAP binding as well as a pivotal phospholipid for DAP CM oligomerization (36–38).

Fourth, quantification of the overall CL content demonstrated that exposure to MEM in DAP-S strains or MEM and LOX in DAP-R strains led to significant increases in overall CM CL. Moreover, the per-cell CL content showed that all β-lactams in DAP-S strains as well as MEM, LOX, and FOX in DAP-R strains led to significantly increased CL contents. Of note, such increases in the CL content could well explain, at least in part, the relative decrease in the positive surface charge that we observed.

A recent study by Jiang et al. found that point mutations in *cls2*, linked to the development of DAP-R, led to increased CL contents in the CM, accompanied by compensatory reductions in the PG content; they further hypothesized that certain DAP-R-associated mutations in the transmembrane region of *cls2* may also lead to changes in the CL distribution (37). However, the latter study focused on laboratory-derived strains with only *cls2*
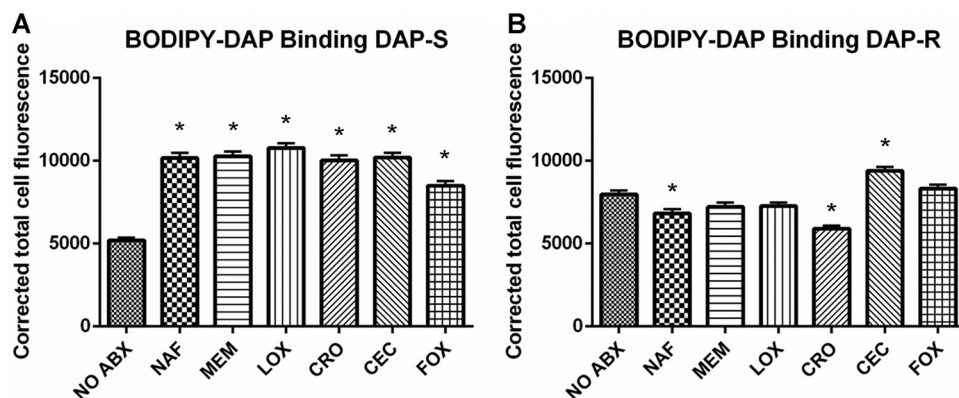
FIG 4 Quantification of the fluorescence intensity of BODIPY-DAP confocal images of DAP-S (A) and DAP-R (B) strains, with or without β-lactam treatment. Average binding ($\pm$ the standard deviation) for DAP-S/DAP-R strains is presented. *, $P < 0.05$ versus no antibiotics.

point mutations with a gain-of-function phenotype. Their investigations did not address clinically derived strains, which likely also contain mutations in other CM homeostasis genes (e.g., in *mprF*, which increases the content of positively charged lysyl-PG, which can potentially repel the active DAP-calcium complex) (25, 39, 40). Thus, the exact mechanism (s) by which the apparent β-lactam-enhanced CL content and redistribution in MRSA contribute to increased DAP activity remains elusive.

Fifth, confocal microscopy suggested that β-lactam exposures resulted in a delocalization of CL away from the divisome and to a more generalized circumferential distribution. There appear to be two potential "competing" outcomes of such CL delocalization. On the one hand, such CL-rich CMs are more susceptible to bending and stretching in terms of dividing due to limited lateral interaction with other phospholipids (37). In such strains, it is possible that this β-lactam-induced CL delocalization might improve DAP's insertion and CM pore formation, enhancing its microbicidal activity. On the other hand, delocalization of CL away from the divisome (a principal site of action) could impede DAP's activity, as noted above for DAP-R enterococci (35).

Sixth, several previous studies looking at DAP–β-lactam combinations suggested that increased DAP binding likely explained the observed synergy (23, 41). However, Berti et al. and Dhand et al. clearly demonstrated that the extent of DAP binding did not uniformly correlate with DAP–β-lactam synergy (20, 23). In support of the latter notion, our current results do not show a consistent relationship between DAP binding and β-lactam exposures; thus, in general, DAP binding was enhanced by β-lactams in DAP-S strains but overall decreased in DAP-R strains. In particular, two of the tested DAP-R strains showed 2-fold decreases in DAP binding following β-lactam exposures, driving down the average reported binding. Previous studies in select strains have shown NAF exposure to increase DAP binding in MRSA (20). However, our more comprehensive strain set analyses demonstrated important strain-to-strain variations and, on average, lower DAP binding after β-lactam exposures in DAP-R strains. We hypothesize that DAP-R strains likely have fundamentally exaggerated responses to β-lactam stress versus DAP-S strains, perhaps in a way that globally decreases DAP binding to CMs (19, 21).

Finally, comparing distinct β-lactams, our data suggest that discrete mechanisms of cellular responses to specific agents underlie DAP–β-lactam synergy in DAP-R strains. For example, NAF exposures led to a decrease in the positive surface charge; this suggested that the β-lactam-mediated reversal of the usual increased surface charge in DAP-R strains is one key synergy mechanism of treatment with NAF plus DAP. In comparison, CRO and FOX yielded decreased surface charge and increased CM rigidity, implying that such a CM profile favors DAP activity. MEM and LOX exposures resulted in increased CL contents, in addition to the reversal of other DAP-R-associated phenotypes. As changes in

TABLE 1 Overview of changes in cell envelope characteristics following β-lactam treatment of DAP-R strains compared to untreated strains and adaptations favorable for DAP activity

Parameter	Value for drug[a]					
	NAF	MEM	LOX	CRO	CEC	FOX
Phenotype						
Surface charge	−	−	−	−	+	−
Membrane fluidity	NC	−	−	−	+	−
CL content, cultures	NC	+	+	NC	NC	NC
CL content, cells	NC	+	+	NC	NC	+
DAP binding	−	NC	NC	−	+	NC
Potential mechanism of DAP potentiation	Decreased surface charge	Decreased surface charge Decreased membrane fluidity Increased CL content	Decreased surface charge Decreased membrane fluidity Increased CL content	Decreased surface charge Decreased membrane fluidity	Increased DAP binding	Decreased surface charge Decreased membrane fluidity

[a]+, increased; −, decreased; NC, no change.

surface charge, CM order, and CL content were noted following MEM or LOX exposure, it is likely that all of these phenotypes play a combinatorial role in DAP synergy. In contrast, CEC conditioning led to a significant increase in DAP binding, suggesting that CEC-DAP synergy is primarily based on the enhancement of DAP binding.

Collectively, our findings imply that the mechanisms underlying interactions between distinct β-lactams and DAP vary from strain to strain, providing an explanation for the broad range of phenotypic responses observed with different DAP–β-lactam combinations.

It should be noted that this study was specifically designed to utilize uniformly bacteriostatic β-lactam concentrations based on in vitro MICs. This strategy yielded supraphysiological β-lactam antibiotic exposures in some instances, which are not achievable in most clinical settings in vivo. Further studies correlating the above-described phenotypic metrics to strain-specific synergy and genetic profiles, employing more clinically relevant β-lactam antibiotic concentrations, are under way.

MATERIALS AND METHODS

Bacterial strains and growth conditions. This study focused on the analysis of nine previously characterized clinical bloodstream DAP-S/DAP-R isogenic MRSA strain pairs (2, 19, 31). These strain pairs were prioritized to include DAP-R strains with or without mprF mutations and have been previously characterized for certain phenotypic and genotypic characteristics (19, 31).

The following β-lactams with wide-ranging PBP selectivity were employed: cloxacillin (LOX) (PBP-1), meropenem (MEM) (PBP-1), nafcillin (NAF) (PBP nonselective), ceftriaxone (CRO) (PBP-2), cefaclor (CEC) (PBP-3), and cefoxitin (FOX) (PBP-4) (42). Exposure concentrations of these β-lactams were chosen based on extensive pilot experiments to determine drug levels for each single antibiotic that exerted a sublethal (bacteriostatic) impact in vitro, defined as a <2-$\log_{10}$-CFU/ml reduction in growth over a 24-h period (see Table S1 in the supplemental material). Bacteriostatic concentrations were selected to compile an overarching analysis of all β-lactam-induced adaptations (rather than using fixed β-lactam concentrations for all strains based on human-achievable serum levels).

Surface charge. The relative net positive cell surface charge was quantified using the spectrophotometrically based cytochrome c binding assay (a highly cationic molecule) as previously described (31, 32). Study strain pairs were grown overnight in the presence or absence of sublethal concentrations of the individual β-lactams listed above. Bacterial suspensions were then centrifuged at 5,000 rpm for 5 min, the supernatant was then removed (containing the β-lactam of interest), and cells were resuspended in fresh medium. Cells were then washed twice with MOPS (morpholinepropanesulfonic acid) buffer (20 mM; pH 7.0), adjusted to an optical density at 600 nm (OD_{600}) of 1.0, and collected from 1-ml aliquots via centrifugation. Cell pellets were resuspended in 200 μl MOPS buffer and combined with 50 μl of cytochrome c (2.5-mg/ml solution). Samples were incubated for 10 min at room temperature and separated by centrifugation. The OD_{530} was determined in the supernatant, and the magnitude of cytochrome c binding was then determined using a standard curve. The more cytochrome c remaining in the supernatant is a measure of a relative increase in the relative bacterial positive surface charge.

Quantification of anionic phospholipids. DAP-S/DAP-R MRSA pairs were grown overnight to stationary phase in the presence or absence of bacteriostatic concentrations of the above-mentioned β-lactams. CL is the principal anionic phospholipid species in the MRSA CM; we utilized an anionic phospholipid-specific dye (N-acrylamide orange [NAO])-based spectrofluorometric assay as a surrogate for CM CL content. As negative controls for this NAO binding assay, we employed the cardiolipin synthase knockout mutants N315 $\Delta cls1$ and N315 $\Delta cls2$ (43) (Fig. S1). For this assay, 1.0×10^7 CFU/ml of each MRSA strain were exposed to 20 μM NAO and then incubated at 4°C for 20 min. The NAO fluorescence intensity was measured using spectrofluorometry (excitation at 525 nm and emission at 640 nm).

Anionic phospholipid localization. Anionic phospholipid localization was visualized using stimulated emission depletion (STED) fluorescence microscopy. Cells were grown to exponential phase with shaking at 37°C in LB medium overnight in the presence or absence of bacteriostatic concentrations of each distinct β-lactam. NAO was then added at 20 μM for 1 h at room temperature. Cells were washed and resuspended in phosphate-buffered saline (PBS). For nucleus staining, 1 μl of NucSpot Live 650 nuclear stain was added to a 1-ml suspension, and the mixture was incubated for 10 min at room temperature. The cells were concentrated 20-fold at the last step, and 3 μl was placed on a glass slide. Slides were set with Prolong diamond antifade mountant and a number 1.5 glass coverslip. Images were collected using a Leica SP8 3× STED superresolution confocal microscope using standard filter sets for either green fluorescent protein (GFP) (495-nm excitation and 510- to 579-nm emission, with 592-nm depletion) to visualize NAO or Cy5 (633-nm excitation and 667- to 742-nm emission, with 775-nm depletion) to visualize NucSpot according to the manufacturer's instructions. Images were processed with Huygens software deconvolution wizard. In addition to CL visualization to identify effects on its CM localization, overall average CL quantification within individual cells was performed by measurement of the integrated fluorescence density in ImageJ for 30 cells in total in the NAO channel, and the corrected cell total NAO fluorescence was then calculated.

CM order (fluidity/rigidity). Strains were grown at 37°C for 72 h in tryptic soy broth (TSB), replacing the medium and β-lactam antibiotic every 24 h, with or without exposure to the average unbound

concentration of each selected β-lactam. CM fluidity/rigidity was then measured using the fluorescent probe 1,6-diphenyl-1,3,5-hexatriene (DPH). Methods for DPH incorporation into the CM, measurement of fluorescence polarization, and calculation of the polarization index have been previously described in detail (44). A BioTek Synergy H1 hybrid multimode reader with excitation at 360 nm and emission at 426 nm was used.

BODIPY-DAP fluorescence microscopy. To quantify DAP binding (in the presence or absence of each β-lactam), cells were harvested at exponential phase from LB cultures supplemented with 50 μg/ml Ca^{2+}. Cells were incubated with 16 μg/ml BODIPY-labeled DAP as previously described (23). The cells were concentrated 20-fold, and 3 μl was placed on a glass slide. Slides were set with Prolong diamond antifade mountant and a number 1.5 glass coverslip. Images were collected using a Leica SP8 3× STED superresolution confocal microscope using a 489-nm laser line and 510- to 579-nm emission, with 660-nm depletion. ImageJ was utilized to measure the integrated fluorescence density of 30 cells, and the corrected cell total fluorescence was calculated.

Statistical analysis. The two-tailed Student t test was used for statistical analysis of β-lactams compared to untreated strains. One-way analysis of variance (ANOVA) was used for β-lactam comparisons.

SUPPLEMENTAL MATERIAL

Supplemental material is available online only.
SUPPLEMENTAL FILE 1, PDF file, 0.2 MB.

ACKNOWLEDGMENTS

REFERENCES

1. Turner NA, Sharma-Kuinkel BK, Maskarinec SA, Eichenberger EM, Shah PP, Carugati M, Holland TL, Fowler VG, Jr. 2019. Methicillin-resistant *Staphylococcus aureus*: an overview of basic and clinical research. Nat Rev Microbiol 17:203–218. https://doi.org/10.1038/s41579-018-0147-4.
2. Fowler VG, Jr, Boucher HW, Corey GR, Abrutyn E, Karchmer AW, Rupp ME, Levine DP, Chambers HF, Tally FP, Vigliani GA, Cabell CH, Link AS, DeMeyer I, Filler SG, Zervos M, Cook P, Parsonnet J, Bernstein JM, Price CS, Forrest GN, Fätkenheuer G, Gareca M, Rehm SJ, Brodt HR, Tice A, Cosgrove SE, S. aureus Endocarditis and Bacteremia Study Group. 2006. Daptomycin versus standard therapy for bacteremia and endocarditis caused by *Staphylococcus aureus*. N Engl J Med 355:653–665. https://doi.org/10.1056/NEJMoa053783.
3. Miller WR, Bayer AS, Arias CA. 2016. Mechanism of action and resistance to daptomycin in *Staphylococcus aureus* and enterococci. Cold Spring Harb Perspect Med 6:a026997. https://doi.org/10.1101/cshperspect.a026997.
4. Bayer AS, Schneider T, Sahl HG. 2013. Mechanisms of daptomycin resistance in *Staphylococcus aureus*: role of the cell membrane and cell wall. Ann N Y Acad Sci 1277:139–158. https://doi.org/10.1111/j.1749-6632.2012.06819.x.
5. Allen NE, Hobbs JN, Alborn WE, Jr. 1987. Inhibition of peptidoglycan biosynthesis in gram-positive bacteria by LY146032. Antimicrob Agents Chemother 31:1093–1099. https://doi.org/10.1128/AAC.31.7.1093.
6. Muthaiyan A, Silverman JA, Jayaswal RK, Wilkinson BJ. 2008. Transcriptional profiling reveals that daptomycin induces the *Staphylococcus aureus* cell wall stress stimulon and genes responsive to membrane depolarization. Antimicrob Agents Chemother 52:980–990. https://doi.org/10.1128/AAC.01121-07.
7. Pogliano J, Pogliano N, Silverman JA. 2012. Daptomycin-mediated reorganization of membrane architecture causes mislocalization of essential cell division proteins. J Bacteriol 194:4494–4504. https://doi.org/10.1128/JB.00011-12.
8. Straus SK, Hancock RE. 2006. Mode of action of the new antibiotic for Gram-positive pathogens daptomycin: comparison with cationic antimicrobial peptides and lipopeptides. Biochim Biophys Acta 1758:1215–1223. https://doi.org/10.1016/j.bbamem.2006.02.009.
9. Scott WR, Baek SB, Jung D, Hancock RE, Straus SK. 2007. NMR structural studies of the antibiotic lipopeptide daptomycin in DHPC micelles. Biochim Biophys Acta 1768:3116–3126. https://doi.org/10.1016/j.bbamem.2007.08.034.
10. Muraih JK, Pearson A, Silverman J, Palmer M. 2011. Oligomerization of daptomycin on membranes. Biochim Biophys Acta 1808:1154–1160. https://doi.org/10.1016/j.bbamem.2011.01.001.
11. Yang SJ, Kreiswirth BN, Sakoulas G, Yeaman MR, Xiong YQ, Sawa A, Bayer AS. 2009. Enhanced expression of *dltABCD* is associated with the development of daptomycin nonsusceptibility in a clinical endocarditis isolate of *Staphylococcus aureus*. J Infect Dis 200:1916–1920. https://doi.org/10.1086/648473.
12. Utaida S, Dunman PM, Macapagal D, Murphy E, Projan SJ, Singh VK, Jayaswal RK, Wilkinson BJ. 2003. Genome-wide transcriptional profiling of the response of *Staphylococcus aureus* to cell-wall-active antibiotics reveals a cell-wall-stress stimulon. Microbiology (Reading) 149:2719–2732. https://doi.org/10.1099/mic.0.26426-0.
13. Rose WE, Schulz LT, Andes D, Striker R, Berti AD, Hutson PR, Shukla SK. 2012. Addition of ceftaroline to daptomycin after emergence of daptomycin-nonsusceptible *Staphylococcus aureus* during therapy improves antibacterial activity. Antimicrob Agents Chemother 56:5296–5302. https://doi.org/10.1128/AAC.00797-12.
14. Jorgensen SCJ, Zasowski EJ, Trinh TD, Lagnf AM, Bhatia S, Sabagha N, Abdul-Mutakabbir JC, Alosaimy S, Mynatt RP, Davis SL, Rybak MJ. 2020. Daptomycin plus β-lactam combination therapy for methicillin-resistant *Staphylococcus aureus* bloodstream infections: a retrospective, comparative cohort study. Clin Infect Dis 71:1–10. https://doi.org/10.1093/cid/ciz746.
15. Rand KH, Houck HJ. 2004. Synergy of daptomycin with oxacillin and other β-lactams against methicillin-resistant *Staphylococcus aureus*. Antimicrob Agents Chemother 48:2871–2875. https://doi.org/10.1128/AAC.48.8.2871-2875.2004.
16. Sakoulas G, Moise PA, Casapao AM, Nonejuie P, Olson J, Okumura CY, Rybak MJ, Kullar R, Dhand A, Rose WE, Goff DA, Bressler AM, Lee Y, Pogliano J, Johns S, Kaatz GW, Ebright JR, Nizet V. 2014. Antimicrobial salvage therapy for persistent staphylococcal bacteremia using daptomycin plus ceftaroline. Clin Ther 36:1317–1333. https://doi.org/10.1016/j.clinthera.2014.05.061.
17. Berti AD, Wergin JE, Girdaukas GG, Hetzel SJ, Sakoulas G, Rose WE. 2012. Altering the proclivity towards daptomycin resistance in methicillin-resistant *Staphylococcus aureus* using combination with other antibiotics. Antimicrob Agents Chemother 56:5046–5053. https://doi.org/10.1128/AAC.00502-12.
18. Mishra NN, Yang SJ, Sawa A, Rubio A, Nast CC, Yeaman MR, Bayer AS. 2009. Analysis of cell membrane characteristics of in vitro-selected daptomycin-resistant strains of methicillin-resistant *Staphylococcus aureus*.

Antimicrob Agents Chemother 53:2312–2318. https://doi.org/10.1128/AAC.01682-08.

19. Mishra NN, McKinnell J, Yeaman MR, Rubio A, Nast CC, Chen L, Kreiswirth BN, Bayer AS. 2011. In vitro cross-resistance to daptomycin and host defense cationic antimicrobial peptides in clinical methicillin-resistant Staphylococcus aureus isolates. Antimicrob Agents Chemother 55:4012–4018. https://doi.org/10.1128/AAC.00223-11.

20. Berti AD, Theisen E, Sauer J-D, Nonejuie P, Olson J, Pogliano J, Sakoulas G, Nizet V, Proctor RA, Rose WE. 2016. Penicillin binding protein 1 is important in the compensatory response of Staphylococcus aureus to daptomycin-induced membrane damage and is a potential target for β-lactam–daptomycin synergy. Antimicrob Agents Chemother 60:451–458. https://doi.org/10.1128/AAC.02071-15.

21. Renzoni A, Kelley WL, Rosato RR, Martinez MP, Roch M, Fatouraei M, Haeusser DP, Margolin W, Fenn S, Turner RD, Foster SJ, Rosato AE. 2017. Molecular bases determining daptomycin resistance-mediated resensitization to β-lactams (seesaw effect) in methicillin-resistant Staphylococcus aureus. Antimicrob Agents Chemother 61:e01634-16. https://doi.org/10.1128/AAC.01634-16.

22. Berti AD, Baines SL, Howden BP, Sakoulas G, Nizet V, Proctor RA, Rose WE. 2015. Heterogeneity of genetic pathways toward daptomycin nonsusceptibility in Staphylococcus aureus determined by adjunctive antibiotics. Antimicrob Agents Chemother 59:2799–2806. https://doi.org/10.1128/AAC.04990-14.

23. Dhand A, Bayer AS, Pogliano J, Yang SJ, Bolaris M, Nizet V, Wang G, Sakoulas G. 2011. Use of antistaphylococcal β-lactams to increase daptomycin activity in eradicating persistent bacteremia due to methicillin-resistant Staphylococcus aureus: role of enhanced daptomycin binding. Clin Infect Dis 53:158–163. https://doi.org/10.1093/cid/cir340.

24. Mishra NN, Bayer AS, Weidenmaier C, Grau T, Wanner S, Stefani S, Cafiso V, Bertuccio T, Yeaman MR, Nast CC, Yang SJ. 2014. Phenotypic and genotypic characterization of daptomycin-resistant methicillin-resistant Staphylococcus aureus strains: relative roles of mprF and dlt operons. PLoS One 9:e107426. https://doi.org/10.1371/journal.pone.0107426.

25. Yang SJ, Mishra NN, Rubio A, Bayer AS. 2013. Causal role of single nucleotide polymorphisms within the mprF gene of Staphylococcus aureus in daptomycin resistance. Antimicrob Agents Chemother 57:5658–5664. https://doi.org/10.1128/AAC.01184-13.

26. Lew C, Mishra NN, Farah S, Zapata B, Bayer AS, Rose WE. 2020. Beta-lactam exposures to methicillin-resistant Staphylococcus aureus involve cell membrane and surface adaptation for daptomycin synergy. Abstr 30th Eur Congr Clin Microbiol Infect Dis (ECCMID), 18 to 21 April 2020, abstr 3855.

27. Cafiso V, Bertuccio T, Purrello S, Campanile F, Mammina C, Sartor A, Raglio A, Stefani S. 2014. dltA overexpression: a strain-independent keystone of daptomycin resistance in methicillin-resistant Staphylococcus aureus. Int J Antimicrob Agents 43:26–31. https://doi.org/10.1016/j.ijantimicag.2013.10.001.

28. Ernst CM, Staubitz P, Mishra NN, Yang SJ, Hornig G, Kalbacher H, Bayer AS, Kraus D, Peschel A. 2009. The bacterial defensin resistance protein MprF consists of separable domains for lipid lysinylation and antimicrobial peptide repulsion. PLoS Pathog 5:e1000660. https://doi.org/10.1371/journal.ppat.1000660.

29. Rose WE, Fallon M, Moran JJM, Vanderloo JP. 2012. Vancomycin tolerance in methicillin-resistant Staphylococcus aureus: influence of vancomycin, daptomycin, and telavancin on differential resistance gene expression. Antimicrob Agents Chemother 56:4422–4427. https://doi.org/10.1128/AAC.00676-12.

30. Werth BJ, Sakoulas G, Rose WE, Pogliano J, Tewhey R, Rybak MJ. 2013. Ceftaroline increases membrane binding and enhances the activity of daptomycin against daptomycin-nonsusceptible vancomycin-intermediate Staphylococcus aureus in a pharmacokinetic/pharmacodynamic model. Antimicrob Agents Chemother 57:66–73. https://doi.org/10.1128/AAC.01586-12.

31. Mishra NN, Bayer AS. 2013. Correlation of cell membrane lipid profiles with daptomycin resistance in methicillin-resistant Staphylococcus aureus. Antimicrob Agents Chemother 57:1082–1085. https://doi.org/10.1128/AAC.02182-12.

32. Mishra NN, Yang SJ, Chen L, Muller C, Saleh-Mghir A, Kuhn S, Peschel A, Yeaman MR, Nast CC, Kreiswirth BN, Crémieux AC, Bayer AS. 2013. Emergence of daptomycin resistance in daptomycin-naïve rabbits with methicillin-resistant Staphylococcus aureus prosthetic joint infection is associated with resistance to host defense cationic peptides and mprF polymorphisms. PLoS One 8:e71151. https://doi.org/10.1371/journal.pone.0071151.

33. Jones T, Yeaman MR, Sakoulas G, Yang SJ, Proctor RA, Sahl HG, Schrenzel J, Xiong YQ, Bayer AS. 2008. Failures in clinical treatment of Staphylococcus aureus infection with daptomycin are associated with alterations in surface charge, membrane phospholipid asymmetry, and drug binding. Antimicrob Agents Chemother 52:269–278. https://doi.org/10.1128/AAC.00719-07.

34. Müller A, Wenzel M, Strahl H, Grein F, Saaki TNV, Kohl B, Siersma T, Bandow JE, Sahl H-G, Schneider T, Hamoen LW. 2016. Daptomycin inhibits cell envelope synthesis by interfering with fluid membrane microdomains. Proc Natl Acad Sci U S A 113:E7077–E7086. https://doi.org/10.1073/pnas.1611173113.

35. Tran TT, Panesso D, Mishra NN, Mileykovskaya E, Guan Z, Munita JM, Reyes J, Diaz L, Weinstock GM, Murray BE, Shamoo Y, Dowhan W, Bayer AS, Arias CA. 2013. Daptomycin-resistant Enterococcus faecalis diverts the antibiotic molecule from the division septum and remodels cell membrane phospholipids. mBio 4:e00281-13. https://doi.org/10.1128/mBio.00281-13.

36. Peleg AY, Miyakis S, Ward DV, Earl AM, Rubio A, Cameron DR, Pillai S, Moellering RC, Jr, Eliopoulos GM. 2012. Whole genome characterization of the mechanisms of daptomycin resistance in clinical and laboratory derived isolates of Staphylococcus aureus. PLoS One 7:e28316. https://doi.org/10.1371/journal.pone.0028316.

37. Jiang J-H, Bhuiyan MS, Shen H-H, Cameron DR, Rupasinghe TWT, Wu C-M, Le Brun AP, Kostoulias X, Domene C, Fulcher AJ, McConville MJ, Howden BP, Lieschke GJ, Peleg AY. 2019. Antibiotic resistance and host immune evasion in Staphylococcus aureus mediated by a metabolic adaptation. Proc Natl Acad Sci U S A 116:3722–3727. https://doi.org/10.1073/pnas.1812066116.

38. Muraih JK, Harris J, Taylor SD, Palmer M. 2012. Characterization of daptomycin oligomerization with perylene excimer fluorescence: stoichiometric binding of phosphatidylglycerol triggers oligomer formation. Biochim Biophys Acta 1818:673–678. https://doi.org/10.1016/j.bbamem.2011.10.027.

39. Yang SJ, Mishra NN, Kang KM, Lee GY, Park JH, Bayer AS. 2018. Impact of multiple single-nucleotide polymorphisms within mprF on daptomycin resistance in Staphylococcus aureus. Microb Drug Resist 24:1075–1081. https://doi.org/10.1089/mdr.2017.0156.

40. Bayer AS, Mishra NN, Chen L, Kreiswirth BN, Rubio A, Yang SJ. 2015. Frequency and distribution of single-nucleotide polymorphisms within mprF in methicillin-resistant Staphylococcus aureus clinical isolates and their role in cross-resistance to daptomycin and host defense antimicrobial peptides. Antimicrob Agents Chemother 59:4930–4937. https://doi.org/10.1128/AAC.00970-15.

41. Ono D, Yamaguchi T, Hamada M, Sonoda S, Sato A, Aoki K, Kajiwara C, Kimura S, Fujisaki M, Tojo H, Sasaki M, Murakami H, Kato K, Ishii Y, Tateda K. 2019. Analysis of synergy between β-lactams and anti-methicillin-resistant Staphylococcus aureus agents from the standpoint of strain characteristics and binding action. J Infect Chemother 25:273–280. https://doi.org/10.1016/j.jiac.2018.12.007.

42. Berti AD, Sakoulas G, Nizet V, Tewhey R, Rose WE. 2013. β-Lactam antibiotics targeting PBP1 selectively enhance daptomycin activity against methicillin-resistant Staphylococcus aureus. Antimicrob Agents Chemother 57:5005–5012. https://doi.org/10.1128/AAC.00594-13.

43. Tsai M, Ohniwa RL, Kato Y, Takeshita SL, Ohta T, Saito S, Hayashi H, Morikawa K. 2011. Staphylococcus aureus requires cardiolipin for survival under conditions of high salinity. BMC Microbiol 11:13. https://doi.org/10.1186/1471-2180-11-13.

44. Bayer AS, Prasad R, Chandra J, Koul A, Smriti M, Varma A, Skurray RA, Firth N, Brown MH, Koo SP, Yeaman MR. 2000. In vitro resistance of Staphylococcus aureus to thrombin-induced platelet microbicidal protein is associated with alterations in cytoplasmic membrane fluidity. Infect Immun 68:3548–3553. https://doi.org/10.1128/IAI.68.6.3548-3553.2000.